

1
2
3
4
5
6
7
8
9
10
11
12
13
14
15
16
17
18
19
20
21
22
23
24

Gaze Bias Differences Capture Individual Choice Behavior

Armin W. Thomas^{†,1,2,3}, Felix Molter^{†,2,3,4}, Ian Krajbich⁵, Hauke R. Heekeren^{2,3}, & Peter N. C. Mohr^{*,2,3,4}

1 Technische Universität Berlin

2 Freie Universität Berlin

3 Center for Cognitive Neuroscience Berlin

4 WZB Berlin Social Science Center

5 Ohio State University

* Corresponding author

† Shared first authorship with equal contribution.

25 Author Note

26 Armin W. Thomas, Electrical Engineering and Computer Science, Technische

27 Universität Berlin; Felix Molter, School of Business & Economics, Freie Universität Berlin;

28 Ian Krajbich, Department of Psychology, Department of Economics, Ohio State University;

29 Hauke R. Heekeren, Department of Education & Psychology, Freie Universität Berlin; Peter

30 N. C. Mohr, School of Business & Economics, Freie Universität Berlin.

31 Ordering of shared first authorship was determined by the following coin toss

32 procedure: A.W.T. brought three Canadian Dollar coins from which F.M. selected one. F.M.

33 chose one of the coin's sides. F.M. flipped the coin and let it fall onto a hard wooden floor.

34 The upper side of the coin then determined the ordering outcome.

35 Correspondence concerning this article should be addressed to Peter N. C. Mohr,

36 School of Business & Economics, Freie Universität Berlin, Garystr. 21, 14195 Berlin,

37 Germany. Email: peter.mohr@neuroeconomics-lab.de.

38 Abstract

39 How do we make simple consumer choices (e.g., deciding between an apple, an
40 orange, and a banana)? Recent empirical evidence suggests a close link between choice
41 behavior and eye movements at the group level, with generally higher choice probabilities for
42 items that were looked at longer during the decision process. However, it is unclear how
43 variable this effect is across individuals. Here, we investigate this question in a
44 multialternative forced-choice experiment using a novel computational model that can be
45 easily applied to the individual participant level. We show that a link between gaze and choice
46 is present for most individuals, but differs considerably in strength, namely, the choices of
47 some individuals are almost independent of gaze allocation, while the choices of others are
48 strongly associated with gaze behavior. Accounting for this variability in our model allows us
49 to explain and accurately predict individual differences in observed choice behavior.

50 *Keywords:* decision making, individual differences, eye movements, gaze bias,
51 evidence accumulation

52 Main text word count: 6506

53

54 Gaze Bias Differences Capture Individual Choice Behavior

55

56 In everyday life, we are constantly confronted with simple consumer choices, such as
57 whether to have an apple or a banana for breakfast, or which bottle of juice to buy at the
58 supermarket. Traditional models describing this type of consumer choice assume that people
59 assign a utility (or subjective value) to each available option and make utility-maximizing
60 choices (Von Neumann & Morgenstern, 1945). Notably, choices are assumed to be based
61 solely on option attributes, and thereby, are independent of information search processes
62 during the decision. This assumption has recently been challenged by a variety of empirical
63 findings showing that the allocation of gaze during the decision-making process also plays a
64 significant role, as a longer gaze towards one option is regularly associated with a higher
65 choice probability for that option (Armel, Beaumel, & Rangel, 2008; Cavanagh, Wiecki,
66 Kochar, & Frank, 2014; Fiedler & Glöckner, 2012; Folke, Jacobsen, Fleming, & De Martino,
67 2016; Glöckner & Herbold, 2011; Konovalov & Krajbich, 2016; Krajbich & Rangel, 2011;
68 Krajbich, Armel, & Rangel, 2010; Krajbich, Lu, Camerer, & Rangel, 2012; Pärnamets et al.,
69 2015; Shimojo, Simion, Shimojo, & Scheier, 2003; Stewart, Gächter, Noguchi, & Mullett,
70 2015; Stewart, Hermens, & Matthews, 2016; Vaidya & Fellows, 2015). Further, external
71 manipulation of an individual's gaze allocation changes choice probabilities accordingly
72 (Armel et al., 2008; Pärnamets et al., 2015; Shimojo et al., 2003; Tavares, Perona, & Rangel,
73 2017).

74 These findings led to the development of novel computational models, which integrate
75 eye movement data into the choice process and formalize the empirically observed association
76 between gaze and choice (Ashby, Jekel, Dickert, & Glöckner, 2016; Cavanagh et al., 2014;
77 Fisher, 2017; Krajbich & Rangel, 2011; Krajbich et al., 2010, 2012; Towal, Mormann, &
78 Koch, 2013). These models are based on classic evidence accumulation models (Ratcliff,
79 1978; Ratcliff, Smith, Brown, & McKoon, 2016) and make the additional assumption that the

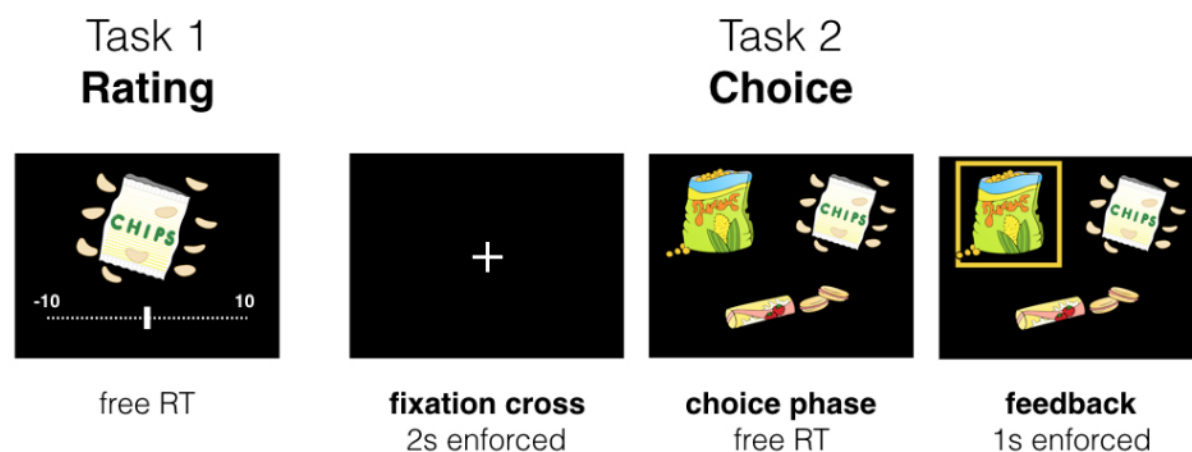
80 momentary rate of evidence accumulation depends on the decision maker's eye movements:
81 Evidence accumulation for an option is assumed to be discounted by a constant factor while
82 another item is fixated upon. Accounting for this gaze bias, these models provide a precise
83 quantitative account of many aspects of simple consumer choice behavior at the group level.

84 While group level statistics are informative for some research questions (e.g.,
85 forecasting product sales in economic research), statements about the majority of people, or
86 the "average person", are often unsuitable for understanding the choice behavior of an
87 individual. Even worse, aggregate models of behavior can lead to false conclusions about true
88 underlying individual processes (Grandy, Lindenberger, & Werkle-Bergner, 2017;
89 Lewandowsky & Farrell, 2010): In a learning task, for example, the group level average
90 learning curve would appear as a gradual, smooth function over time, even if all individuals
91 showed abrupt, step-like learning curves (much like an epiphany), but with variable learning
92 onsets across individuals (Hayes, 1953). This group level model, however, would not describe
93 any individual of the group well, and the deduction that individual learning occurs smoothly
94 would be false. It is thus crucial to understand and explain choice behavior at the individual
95 level.

96 Similarly, previously reported group level models quantifying the association between
97 gaze and choice specified a constant gaze bias for all individuals (e.g., Krajbich et al., 2010;
98 Krajbich & Rangel, 2011), without testing the model performance on the individual level. It
99 therefore remains to be shown whether an association between gaze and choice is present
100 across individuals and whether the strength of such an association is constant. If, however,
101 people's decisions were affected differently by looking behavior, we would find that the
102 choices of some individuals are more biased by gaze, and therefore, more inconsistent with
103 subjective value ratings than other individuals' choices. Imagine, for example, a choice
104 between two bottles of orange juice in the supermarket: one has a slightly higher utility for the
105 decision maker than the other, but it is also less visually salient. If this person's association of

106 gaze and choice behavior was strong, her choice would be biased towards the bottle that is
107 attracting more of her gaze, even though it has lower utility. On the other hand, if the person's
108 association is weak, she would then be able to select the option that is higher in utility, despite
109 her gaze being attracted more towards the inferior option. Accordingly, if the strength of this
110 association is variable across individuals, it is necessary to account for these differences to
111 accurately predict individual choice behavior.

112 Here, we investigated whether the previously reported link between gaze and choice
113 behavior is variable across individuals, using a novel computational model that can easily be
114 applied to individual participant and multialternative choice data. With this model, we
115 reaffirmed that an association between gaze and choice is present at the group level, and
116 indeed, present for most individuals. The strength of this association, however, showed
117 substantial variability. By accounting for this variability, we were able to explain and
118 accurately predict empirically observed differences in individuals' choice behavior.



119

120 *Figure 1: Experimental Paradigm. All the participants completed two tasks in a single*

121 session. **Task 1:** The participants rated all 70 snack foods items on a liking rating scale

122 between -10 and 10, according to how much they would like to eat each item. **Task 2:** In each

123 choice trial, the participants were required to maintain a central fixation for 2 s. Next, the

124 participants were asked to choose the item that they would like to eat most from sets of 3

125 choice items, while their eye movements were being recorded. Choices were followed by 1 s

126 of visual feedback.

127

Results

Data set & Task overview

129 To investigate individual differences in the influence of gaze allocation on simple

130 economic choice behavior, we used a previously published, prototypical data set (Krajbich &

131 Rangel, 2011) that we obtained from the original authors in a preprocessed format (see

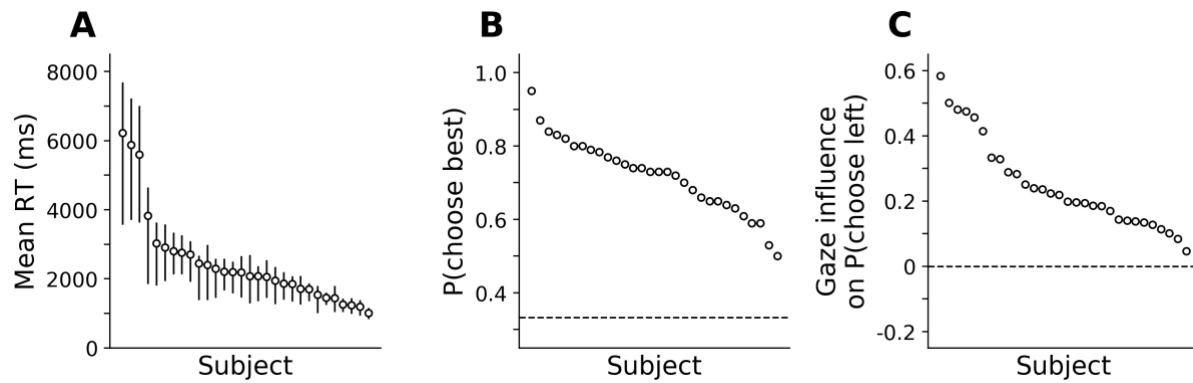
132 [Methods](#) for full details). In the corresponding experiment, hungry participants made choices

133 between three snack food items, without time restrictions ([Figure 1](#)). Participants also gave a

134 liking rating for each of the 70 snack food items that were used in the experiment. During the

135 choice task, the participants' eye movements were continuously recorded using an eye

136 tracker. The data set included 30 participants, who performed 100 choice trials each.



137

138

139

140

141

142

143

144

145

146 **Individual differences in the data**

147

148

149

150

151

152

153

154

155

Figure 2: Individual differences in the three behavioral metrics: response time,

*probability of choosing the highest rated item and influence of gaze on choice probability. **A:***

*Mean individual response times (error bars denote first and third quartile). **B:** Mean*

probability of choosing the item with the highest liking rating. The dashed horizontal line

*indicates chance level accuracy. **C:** Individual influence of gaze on choice probability (mean*

increase in choice probability for an item that is fixated longer than the others, after correcting

for the influence of item value). The data points are sorted from high to low in each panel.

We analyzed three metrics for individual differences, namely, (i) the participants'

response time, (ii) the mean probability of choosing the item with the highest liking rating,

and (iii) the influence of gaze allocation on choice probability (mean increase in choice

probability for an item that was fixated on longer than the others, after correcting for the

influence of the item value). We found that participants differed considerably in all of the

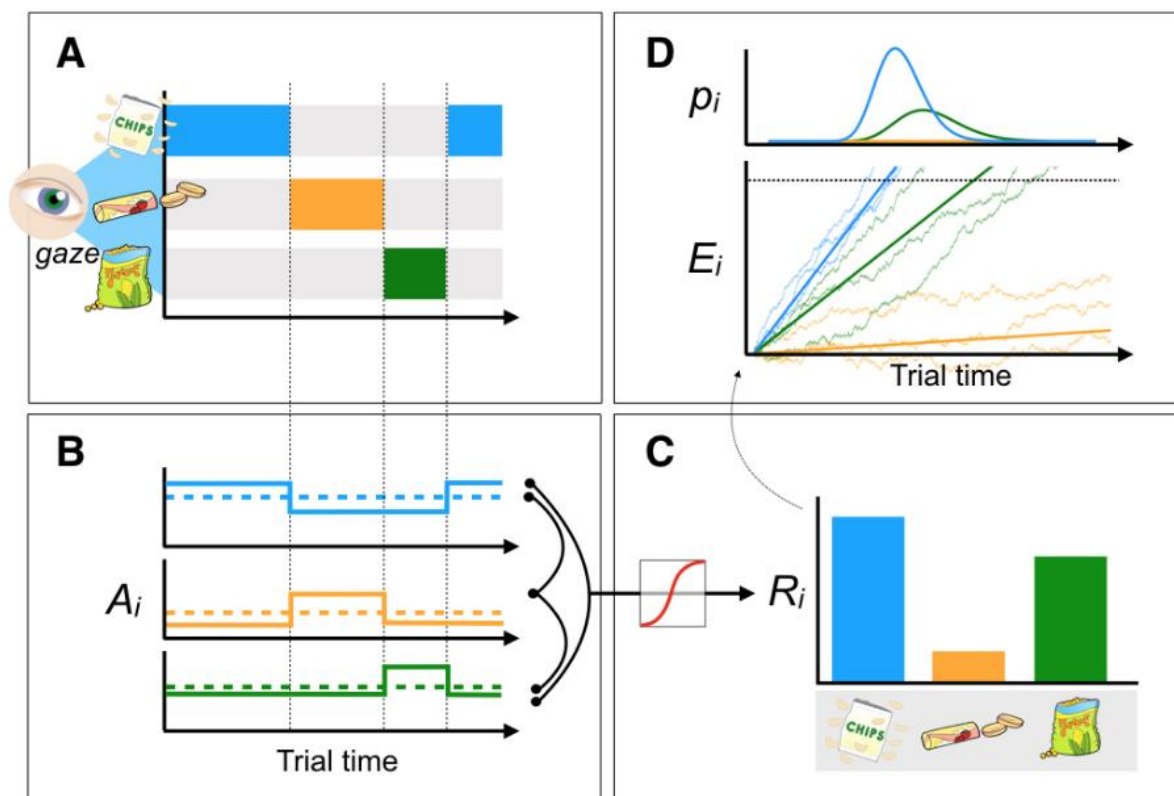
three metrics (Figure 2):

The participants' mean response times ranged from 1006 to 6217 ms, with mean \pm s.d.

$= 2462 \pm 1298$ ms (Figure 2A), while their probabilities of choosing the highest rated item in

a trial ranged from 50.00% to 95.00%, with mean \pm s.d. $= 71.94\% \pm 10.01\%$ (Figure 2B).

156 We also probed the relationship between individual allocation of gaze and choice.
157 Previous work in simple choice tasks has shown that individuals are, on average, more likely
158 to choose an option when they spent more time fixating on it, relative to the others (Armel et
159 al., 2008; Cavanagh et al., 2014; Folke et al., 2016; Krajbich & Rangel, 2011; Krajbich et al.,
160 2010). Here, we devised an individual measure to quantify the relationship between gaze
161 allocation and choice for each individual: following previous work (Krajbich & Rangel, 2011;
162 Krajbich et al., 2010), for each participant we first estimated the probability of choosing the
163 left item in a choice set using logistic regression, based on its relative item value (the
164 difference between the item's value and the mean value of all other items in that trial) and the
165 range between the other items' value. We then subtracted this estimated probability from the
166 empirically observed choice (either 1 if the left item was chosen, or 0 otherwise). Finally, we
167 averaged the resulting "residual" choice probability for trials in which the left item had a
168 positive and negative final gaze advantage (computed as the difference in the fraction of the
169 total fixation time that the participants spent fixating on the left item and the average fraction
170 that they spent fixating on the others). The difference between these two described the
171 average difference in choice probability for the items with a positive versus negative final
172 gaze advantage, when corrected for the influence of relative item value on choice probability
173 and the other items' range of values. We found that individual scores on this measure ranged
174 from 0.05 to 0.58, with mean \pm s.d. = 0.25 ± 0.14 (Figure 2C). Notably, all the participants
175 showed positive scores, indicating an overall positive relationship between gaze allocation
176 and choice. We did, however, find strong variation in this measure.



177
 178 *Figure 3: Gaze-weighted linear accumulator model (GLAM). The GLAM describes*
 179 *the influence of gaze allocation on the decision process, in the form of a linear stochastic race:*
 180 *It assumes that individuals accumulate evidence in favor of each item i and make a choice as*
 181 *soon as the relative evidence E_i in favor of one item reaches a choice threshold (D).*
 182 *Importantly, the speed of the accumulation process is dependent on the distribution of visual*
 183 *gaze during the decision (A & B). For each option in the choice set, an absolute evidence*
 184 *signal A_i is computed. The magnitude of this signal is dependent on the allocation of visual*
 185 *gaze, with lower magnitudes for options that are momentarily not fixated on. Absolute*
 186 *evidence signals are transformed into relative decision signals R_i (indicating relative item*
 187 *preferences) by (i) computing the average absolute evidence signal for each item in the trial*
 188 *(dashed lines in B), (ii) and then computing the difference between each of these averages and*
 189 *the maximum of the respective other two. (iii) The GLAM assumes an adaptive representation*
 190 *of these relative evidence signals that is maximally sensitive to small differences in the*
 191 *relative decision signals. To this end, a sigmoid transform is applied (C). The resulting scaled*

192 relative evidence signals determine the drift terms R_i in the stochastic race (**D**). The stochastic
193 race provides first-passage time distributions p_i , describing the likelihood of each item being
194 chosen at each time point. See [Methods](#) for a more detailed model description.

195

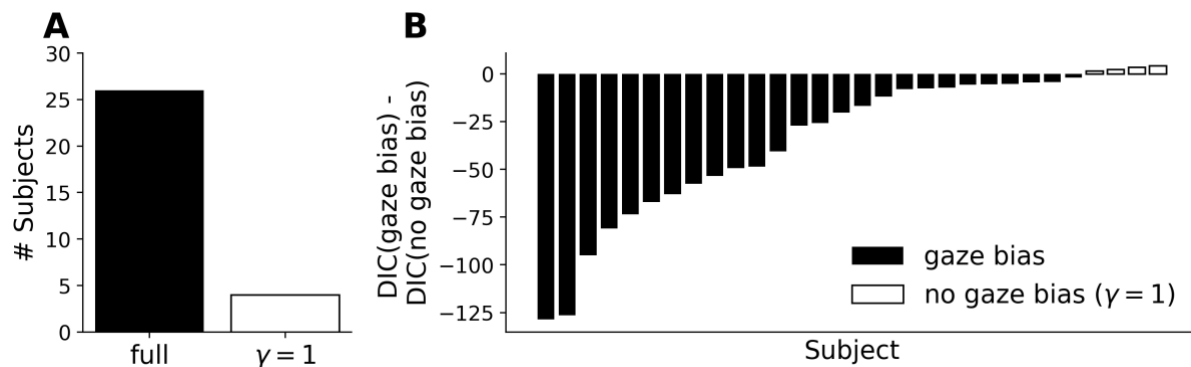
196 **Modeling individual differences in simple economic choice**

197 The behavioral and eye tracking data suggest substantial variability in the extent to
198 which gaze affects a participant's choice behavior ([Figure 2C](#)). The computational mechanism
199 relating gaze and choice patterns, however, cannot be inferred from descriptive analyses
200 alone. In addition, conclusive quantitative evidence for or against the presence of a
201 mechanism that biases choices depending on the distribution of gaze has yet to be provided at
202 the individual level. We therefore adopted a principled computational modeling approach to
203 investigate whether a formalized gaze bias mechanism, in conjunction with individual gaze
204 patterns, can improve model predictions of individual choice and response time data.

205 We propose a new model called the Gaze-weighted Linear Accumulator Model
206 (GLAM; [Figure 3](#)) that is inspired by the attentional Drift Diffusion Model (aDDM) proposed
207 by Krajbich et al. (2010; also, Krajbich & Rangel, 2011; Krajbich et al., 2012). The GLAM
208 assumes accumulation of evidence in favor of each item, that is modulated by gaze behavior:
209 While an item is not fixated on, accumulation occurs at a rate discounted by the gaze bias
210 parameter γ . A choice is made as soon as evidence in favor of one item reaches a decision
211 threshold. The GLAM is rooted in the class of linear stochastic race models (Tillman, 2017;
212 Usher, Olami, & McClelland, 2002). These models naturally generalize to choice scenarios
213 with more than two items and remain analytically tractable, allowing for more complex
214 applications (e.g., embedding in a hierarchical Bayesian framework).

215 In addition to the gaze bias parameter γ , the GLAM includes a general velocity
216 parameter v , a noise parameter σ and a scaling parameter τ (see [Methods](#) for full model
217 implementation details).

218



220

220 *Figure 4: Model comparison between the full GLAM model and a no-gaze-bias*

221 *GLAM ($\gamma = 1$) variant. A: Individual best fitting models, given by the lowest DIC score.*

222 *Twenty-six of 30 participants (87%) were better described by the full model that includes a*
223 *gaze bias mechanism. B: Individual differences in the Deviance Information Criteria (DIC)*

224 *between the full and ($\gamma = 1$) model. Negative differences in the model DIC scores indicate*
225 *better fits of the full model.*

226

227 **Individual model comparison**

228 We fitted and compared two GLAM variants to the response time and choice data of
229 each participant to gauge the evidence in favor of the previously described gaze bias
230 mechanism and to quantify its strength on an individual level:

231 1. A *full* GLAM variant with free parameters v , γ , σ , τ . This model allowed the gaze
232 bias parameter γ to vary freely between the individuals.

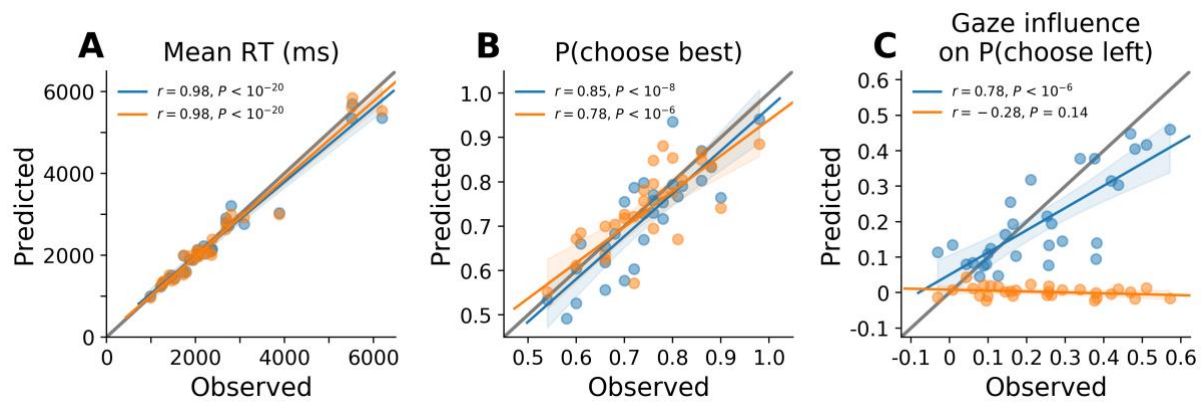
233 2. A *no-gaze-bias* GLAM variant, where the gaze bias parameter γ was fixed to 1
234 (resulting in no influence of gaze on the accumulation process)

235 The two models differ in their complexity: The full model has one more free parameter and
236 can therefore be expected to provide a better absolute fit to the data. We used the Deviance
237 Information Criterion (DIC; Spiegelhalter, Best, Carlin, & Van Der Linde, 2002;
238 Spiegelhalter, Best, Carlin & Van Der Linde, 2014) to perform model comparisons at the
239 individual level as it includes a penalty for model complexity: more complex models are only
240 preferred only if their added complexity is justified by an improvement in absolute fit. Lower
241 DIC scores indicate a better model fit accounting for differences in model complexity.

242 The full model fitted 26 of 30 (87%) participants better than the no-gaze-bias model
243 (Figure 4A, B). The mean \pm s.e.m. difference in the DIC scores between the full and no-gaze-
244 bias models was -34.22 ± 6.84 (Figure 4B).

245 Individual estimates of the gaze bias parameter γ in the full model ranged from -0.93
246 to 0.81, with a mean \pm s.d. = 0.20 ± 0.39 (Figure S2). Notably, the individual estimates
247 covered a wide range of possible values between $\gamma = -1$ (strong gaze bias) to $\gamma = 1$ (no gaze
248 bias). With a strong gaze bias, the GLAM leaks evidence for an item, while another is fixated
249 on, whereas evidence accumulation is independent of gaze allocation when no gaze bias is
250 present.

251 Taken together, the individual model comparison revealed that most participants'
252 behavior was better described by a model that includes the gaze bias mechanism. Importantly,
253 the extent to which the accumulation process was influenced by gaze, as captured by
254 individual gaze bias (γ) estimates, showed non-trivial individual differences.



255

256

Figure 5: Out of sample correlations between the observed and predicted individual

257 *behavior in the odd experiment trials (the predictions were based on parameters estimated*

258 *from even experiment trials). **A:** mean response time. **B:** probability of choosing the highest*

259 *rated item. **C:** influence of gaze on choice probability. Model predictions are simulated from*

260 *hierarchically estimated parameter estimates. Blue color indicates predictions from the full*

261 *GLAM, whereas orange indicates predictions from a restricted GLAM variant with no gaze*

262 *bias ($\gamma = 1$).*

263

264 **GLAM predicts individual choice behavior**

265 We found that in a relative model comparison the full GLAM best describes the data

266 of most participants, when compared to a restricted variant with no gaze bias ($\gamma = 1$; see

267 [Figure 4](#)). However, this analysis did not take into account whether the GLAM also accurately

268 predicts individuals' behavior on an absolute level. To test this, we again used both model

269 variants to simulate response data for each individual participant. This time, however, we split

270 the data into even- and odd-numbered trials. We then used all the even trials to estimate the

271 model parameters (training). Subsequently, we predicted the choices and response times for

272 all the odd-numbered trials (test). The purpose of this out of sample prediction was to validate

273 the individually estimated parameters, by comparing the GLAM's predictions to response

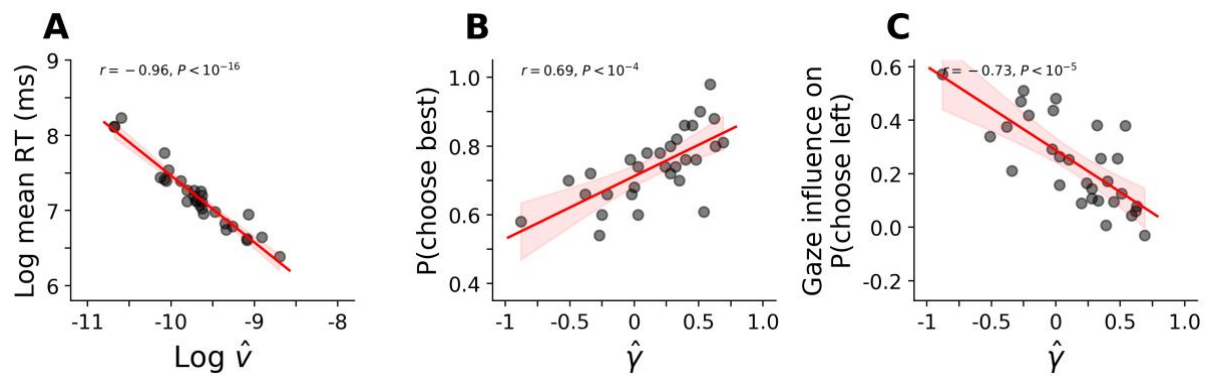
274 data that did not inform the parameter estimates. To compensate for the resulting loss of

275 training data we fitted both GLAM variants using a hierarchical Bayesian framework
276 (Kruschke, 2014; Wiecki, Sofer, & Frank, 2013). Here, individual model parameters and their
277 group distributions are simultaneously estimated from the data. This is desirable as individual
278 parameter estimates are informed by their distribution at the group level, thereby capitalizing
279 on the information that is shared across individuals. With the hierarchical parameter estimates
280 we then tested whether individual behavioral patterns across the three metrics are accurately
281 predicted by the two models (see Figures 2 & 5).

282 We found that the full GLAM variant accurately predicted individual differences in
283 response times ($\beta = 1.06$, $t(28) = 26.17$, $P < 10^{-20}$; Figure 5A). Similarly, individual
284 differences in the probability of choosing the highest rated item were predicted precisely ($\beta =$
285 0.75 , $t(28) = 8.57$, $P < 10^{-8}$; Figure 5B). Lastly, we also found that the full GLAM predicted
286 individual differences in the influence of gaze on choice probability well ($\beta = 0.98$, $t(28) =$
287 6.69 , $P < 10^{-6}$; Figure 5C).

288 The restricted GLAM variant with no gaze bias predicted the participants' individual
289 response times and the probability of choosing the highest rated item similarly well (RT: $\beta =$
290 1.02 , $t(28) = 27.07$, $P < 10^{-20}$, Figure 5A; P(choose best): $\beta = 0.75$, $t(28) = 6.53$, $P < 10^{-6}$,
291 Figure 5B). However, the model failed to predict the influence of gaze on the participants'
292 choices ($\beta = -2.97$, $t(28) = -1.53$, $P = 0.14$; Figure 5C), resulting in no correlation between
293 the predicted and empirical data in our gaze influence measure.

294 These results showed that the full GLAM outperformed the restricted model variant in
295 accurately predicting the participants' empirical choices, as it also captured empirical choice
296 patterns that are driven by gaze and not solely by the items' liking rating.



297

298 *Figure 6: Correlations between individuals response behavior in the odd-numbered*
299 *trials and the model parameters estimated from the even-numbered trials. A: Response time*
300 *and v (plotted on a log-log-scale). B: Probability of choosing the highest rated item and γ . C:*
301 *Influence of gaze on choice probability (mean increase in choice probability for an item that*
302 *is fixated on longer than the others, when corrected for the influence of the item's relative*
303 *value and the range of the other items' values) and γ .*

304

305 **GLAM explains individual choice behavior**

306 We found that the GLAM accurately predicted individuals' response behavior. Next,
307 we tested whether the individual model parameters are able to explain variability in the
308 participants' choice behavior. Here, we used standard OLS regressions to predict the three
309 behavioral metrics in the odd-numbered trials from the individual GLAM parameters that
310 were previously estimated hierarchically from the even-numbered trials (see Figure 6). We
311 found that v (velocity parameter; see Methods for details) scaled logarithmically with the
312 participants mean response time ($\beta = -0.89$, $t(28) = -18.87$, $P < 10^{-16}$; Figure 6A). We did not
313 find a meaningful relationship between the individual σ estimates and the probability of
314 choosing the highest rated item ($\beta = -1.59$, $t(28) = -0.19$, $P = 0.85$), even though the σ
315 parameter determines the magnitude of noise in the accumulation process (see Methods for
316 details). However, we found that γ (gaze bias) estimates predicted the participants'

317 probabilities of choosing the highest rated item ($\beta = 0.18$, $t(28) = 4.98$, $P < 10^{-4}$; [Figure 6B](#)),
318 so that stronger gaze biases (smaller γ) were associated with more choices that were
319 inconsistent with the item ratings. This relationship can be explained as follows: the gaze bias
320 parameter γ allows the model to bias the choice process according to the distribution of gaze
321 between items: with a strong gaze bias, the model's predictions are strongly dependent on the
322 distribution of gaze, and a gaze distribution that is random with respect to the items' liking
323 ratings then leads to random choices. On the other hand, the model's predictions are
324 independent of gaze when no gaze bias is present. The model then neglects gaze and predicts
325 choices solely driven by liking ratings. Lastly, as expected, we also found that γ estimates
326 predicted the participants' individual scores of gaze influence on choice probability ($\beta =$
327 -0.31 , $t(28) = -5.68$, $P < 10^{-5}$; [Figure 6C](#)).

328

329

Discussion

330 Here, we investigated individual differences in the influence of gaze allocation on
331 simple economic choice behavior by analyzing a previously published data set, where
332 individuals made choices between three snack food items. We found that individuals showed
333 an overall positive relationship between gaze and choice (longer gaze increases choice
334 probability), but that the strength of this relationship was highly variable across individuals.
335 To better understand the computational mechanism underlying this effect and its variability,
336 we proposed a new model called the Gaze-weighted Linear Accumulator Model (GLAM). It
337 assumes that individuals accumulate evidence in favor of each available item and make a
338 choice as soon as the cumulative evidence for one item reaches a choice threshold.
339 Importantly, the accumulation process is biased by gaze behavior, with discounted
340 accumulation rates for unattended items. We found that the GLAM accurately predicts
341 individuals' choice and response time data and does so better than a model that does not
342 assume any influence of gaze allocation on choice. We also found that the GLAM's gaze bias

343 estimates reliably explained individual differences in choice behavior, namely, the strength of
344 the individuals' association of gaze and choice behavior and the individuals' probability of
345 choosing the highest rated item in a choice set (stronger gaze biases were generally associated
346 with more choices that were inconsistent with item ratings).

347 With the GLAM, we have provided a model that captures individual choice behavior
348 in simple economic choice tasks with multiple alternatives with high predictive accuracy by
349 integrating information about the individuals' allocation of gaze. It is statistically and
350 computationally tractable, making it readily extendable to novel choice tasks and research
351 questions.

352 Our individual model comparison revealed the added value of a gaze bias mechanism
353 in decision models. The large majority of the participants were better described by the full
354 model, compared to a restricted variant without any influence of gaze on choice. One reason
355 for this superior performance is that the GLAM's use of the individual trial gaze data allows
356 the model to make different predictions across otherwise identical choice sets. In this way, the
357 model is able to explain variance in behavior that would otherwise be attributed to unspecified
358 decision noise. As decision making can be seen as a stochastic process (Rieskamp, 2008),
359 choices across identical trials with high difficulty (where ratings for the available items are
360 very similar, for example, 3, 2 and 2 for the left, middle and right item, respectively) can be
361 assumed to vary. A stochastic choice model without a gaze bias mechanism will make
362 probabilistic, but identical predictions for two such trials (Gluth & Rieskamp, 2017).
363 Leveraging a gaze bias mechanism, however, allows a model to make trial specific
364 predictions, and these, relying on the generally positive relationship between gaze and choice,
365 will have higher accuracy. We expect the gaze bias mechanism to be especially relevant in
366 high-difficulty trials, where item rating information by itself provides little evidence in favor
367 of any one alternative.

368 Naturally, the inclusion of gaze information into choice models leads to the question
369 of what drives gaze during choice. This question has received considerable attention in
370 previous research, confirming influences of item surface size (Lohse, 1997; Wedel & Pieters,
371 2008), position (Chandon, Hutchinson, Bradlow, & Young, 2009) and saliency (Itti & Koch,
372 2000) on gaze. Still, a formal integration with computationally formalized choice models was
373 achieved only recently (Towal et al., 2013). We believe that the development of generative
374 models for the fixation process itself, and their integration with choice models, has the
375 potential to largely improve existing models.

376 Our analyses also confirmed the need for individual model fits: we found substantial
377 variability across individuals in the influence of gaze on choice that was hidden in the group
378 level analyses. Given that the influence of gaze on choice is variable between participants, a
379 single gaze bias parameter γ for the whole group would not fit all the individuals well and
380 would therefore result in inferior predictive performance of the model: participants whose link
381 between gaze allocation and choice behavior is weaker than the group average would falsely
382 be predicted to make choices less consistent with their value ratings, and driven more by
383 looking behavior. Predictions for the participants' choices with a stronger link than the group
384 average, on the other hand, would not contain enough influence of gaze. Accounting for
385 individual differences in the link between gaze allocation and choice behavior opens
386 important avenues for future research, focusing on the specific determinants of these
387 differences. For example, are these differences best characterized as a trait (stable within a
388 person, but variable between persons), state (variable within a person, between different
389 situations or contexts) or both (variable between persons and contexts) (see Peters & Büchel,
390 2011, for a similar discussion in the context of delay discounting)?

391 Despite a wealth of findings exploring the computational mechanisms underlying
392 simple choice behavior and its link to visual fixations (e.g., Shimojo et al., 2003; Armel et al.
393 2008; Krajbich et al., 2010; Krajbich & Rangel, 2011; Towal et al., 2013; Cavanagh et al.,

394 2014; Fisher, 2017), most of this work, and the associated computational frameworks (e.g.,
395 Ratcliff et al., 2016), is difficult to extend to complex choice scenarios (i.e., involving more
396 than two choice alternatives). Here, we have shown that the GLAM captures individuals'
397 choice behavior well in choice situations with only few choice alternatives. However, the
398 GLAM naturally extends to choices involving many more options, as we mostly encounter in
399 our everyday lives. Imagine standing in front of a vending machine to buy a snack. These
400 machines can easily store up to 20 items. We assume that in these multialternative choice
401 situations, both gaze and individual differences will play an even more prominent role:
402 individuals, when confronted with large choice sets, do not always look at all available items
403 (e.g., Reutskaja, Nagel, Camerer, & Rangel, 2011). A choice model that considers
404 individuals' liking values only will therefore fail in accurately predicting individuals' choice
405 behavior. A model that includes information about individuals' gaze distribution during
406 decision formation will, on the other hand, outperform such naive models, because it will
407 better account for the set of items that individuals actually consider for a choice. In addition,
408 we assume that behavioral differences between individuals to increase with increasing choice
409 set size. For example, we assume that some individuals may look at only a few of the
410 available items, before making a choice, while others may spend a long time searching for the
411 most highly valued option (as indicated in Reutskaja et al., 2011). To understand whether
412 there is a common choice mechanism underlying these different types of choice behavior, it is
413 necessary to test the ability of a model to capture individual choice patterns.

414 Real life choices have another level of complexity often not considered in simple
415 economic choice tasks; options comprise multiple, oftentimes orthogonal attributes. For
416 example, each item in a vending machine is associated with a price that has to be considered.
417 Consumer goods often also include other attributes (e.g., ratings by other consumers: De
418 Martino, Bobadilla-Suarez, Nouguchi, Sharot, & Love, 2017; energy consumption, etc.),
419 which are commonly displayed visually to the decision maker. Certain configurations of

420 option attributes can induce systematic shifts in preference, called context effects (Mohr,
421 Heekeren, & Rieskamp, 2017; Soltani, De Martino, & Camerer, 2012; Trueblood, Brown,
422 Heathcote, & Busemeyer, 2013). These preference shifts can vary considerably between
423 individuals (Mohr et al., 2017). Notably, eye-tracking data about the identity and sequence of
424 fixated attributes are predictive of choice in context effect settings (Noguchi & Stewart,
425 2014). Future research on these effects and their relationship to gaze requires a model that can
426 be fitted on an individual basis and is applicable to multialternative choice scenarios. The
427 GLAM provides a starting-point to explore these types of research questions in the future.

428 Like other existing decision making models (e.g., Usher and McClelland, 2001; Roe,
429 Busemeyer & Townsend, 2001; Ratcliff et al., 2016; Krajbich et al., 2010), the GLAM also
430 incorporates several assumptions about the neural computations underlying simple economic
431 choices. It is necessary to evaluate the plausibility of these assumptions, next to the ability of
432 a model to capture individuals' choice behavior. The GLAM assumes evidence accumulation
433 towards a decision threshold and a fixation-dependent bias of this process. There is strong
434 neural evidence for accumulation-to-bound processes during decision formation in a variety
435 of choice tasks (e.g., Basten, Biele, Heekeren, & Fiebach, 2010; Philiastides & Sajda, 2007;
436 Churchland, Kiani & Shadlen, 2008; Liu & Pleskac, 2011; O'Connell, Dockree & Kelly,
437 2012; Wyart, De Gardelle, Scholl & Summerfield, 2012; Polanía, Krajbich, Grueschow &
438 Ruff, 2014; Lafuente, Jazayeri & Shadlen, 2015; for a review see Gold & Shadlen, 2001, and
439 Heekeren, Marrett & Ungerleider, 2008). Recently, it was also shown that single-trial EEG
440 components reflecting attention in simple perceptual decision-making tasks explain variance
441 in single-trial evidence accumulation rates of the decision process (Nunez, Vandekerckhove,
442 & Srinivasan, 2017) and that variability in these components can explain behavioral
443 differences between individuals (Nunez, Srinivasan, & Vandekerckhove, 2015). Two recent
444 studies also provided first empirical evidence that value-driven activity in the orbitofrontal
445 cortex of monkeys is modulated by fixation location when they viewed reward-associated

446 visual cues in a free-viewing paradigm (Hunt, Malalasekera, Berker, Miranda, Farmer,
447 Behrens & Kennerley, 2017; McGinty, Rangel, & Newsome, 2016). Together, these studies
448 provided the first neurobiological evidence of the influence of visual fixations on the process
449 of decision formation. Ultimately, a better understanding of these computations will be central
450 to building holistic models of the choice process and for advancing existing choice
451 frameworks. In addition, it might also help us to better understand the origin of behavioral
452 variability that we observe within and between individuals.

453 The focus on individual differences in the relationship between gaze and choice
454 behavior can also prove itself relevant in clinical research domains. Increasingly prevalent
455 clinical conditions, such as type 2 diabetes and obesity, typically involve maladaptive
456 decision-making between visually presented stimuli, often strategically positioned and
457 designed to capture attention. Snack food items, for example, are advertised with bright,
458 salient colors and placed prominently (e.g., at eye level, near the checkout in the
459 supermarket), which could have adverse effects on individuals prone to making maladaptive
460 food choices. Healthier diets (i.e., food choices) are both prevention and treatment for such
461 diseases, and a better understanding of how individuals' decisions are impacted by looking
462 behavior could help inform the search for predictors of clinical behavior and improve
463 therapeutic approaches. In addition, individually tailored therapeutic approaches, based on a
464 better understanding of individual response patterns, promise higher efficacy and, in turn,
465 reduced health care spending.

466

467 **Methods**

468 **Data, tasks, procedure & preprocessing**

469 We reanalyzed a data set that was previously published in Krajbich and Rangel
470 (2011). In the corresponding experiment, hungry participants made repeated choices between

471 multiple snack food items (e.g., Twix, Lays Chips, Skittles, etc.), while their eye movements
472 were recorded.

473 The data set contains data from 30 Caltech students, who reported to regularly eat the
474 snack foods that were used in the experiment and had no dietary restrictions. The participants
475 received a show-up fee of \$20 and one food item. The experiment was approved by Caltech's
476 Human Subjects Internal Review Board.

477 All participants were asked not to eat for 3 hours prior to the experiment. In an initial
478 liking rating task the participants indicated liking ratings between -10 to 10 for each of the 70
479 different snack food items using an on screen slider with a randomized starting point and free
480 response time ("How much would you like to eat this at the end of the experiment?"; [Figure](#)
481 [1](#), Task 1). These ratings were used as a measure of the value participants placed on each
482 item. In the subsequent choice task the participants made choices between triplets of food
483 items. The items were arranged in a triangular fashion on the screen ([Figure 1](#), Task 2). In one
484 half of the trials, this triangle pointed upwards (center option on top), in the other half it
485 pointed downwards (center option at the bottom). Choices were indicated with free response
486 times and using the left, down and right arrow keys on a keyboard. Each trial began with a 2 s
487 forced fixation towards the center of the screen. A yellow feedback box was shown around the
488 chosen item for 1 s after a choice was made. Lastly, the participants were required to stay for
489 30 min after the experiment, to eat a food item that they chose in one randomly selected
490 choice trial. The participants performed 100 choice trials each.

491 The participants' eye movements were continuously recorded with a 50 Hz desktop-
492 mounted Tobii eye tracker.

493 The data were obtained from the original authors in an already preprocessed format.
494 The original preprocessing steps included the removal of trials with missing fixation data for
495 more than 500 ms at the beginning or end of the trial, resulting in a total of 2966 remaining
496 trials (mean \pm s.e.m. number of trials dropped per participant was 1.1 ± 0.9). Rectangular

497 areas of interest (AOIs) were constructed around each food item in each trial and visual
498 fixations were assigned to the corresponding item or coded as non-item fixations. If a non-
499 item fixation was preceded and succeeded by fixations on the same item, the non-item fixation
500 would also be assigned to this item. Other non-item fixations were not reassigned and
501 discarded from all further analyses.

502

503 **Gaze-weighted Linear Accumulator Model (GLAM) details**

504 The GLAM belongs to the class of linear stochastic race models (Usher &
505 McClelland, 2001). It assumes accumulation of noisy evidence in favor of each available
506 alternative i , and that the choice is determined by the first accumulator that reaches a common
507 boundary. In particular, we define the accumulated relative evidence E_i in favor of alternative
508 i , as a stochastic process that changes at each point in time t according to:

$$509 \quad E_i(t) = E_i(t - 1) + v \times R_i + N(0, \sigma^2); E_i(0) = 0 \quad (1)$$

510 E_i consists of two separate components: a drift term R_i and zero-centered normally
511 distributed noise with standard deviation σ . The overall speed of the accumulation process is
512 governed by the velocity parameter v . The drift term R_i describes the average amount of
513 relative evidence for item i that is accumulated at each point in time t . We define the relative
514 evidence R_i^* as the difference in the stationary absolute evidence signal A_i of item i and the
515 maximum absolute evidence of all other items J :

$$516 \quad R_i^* = A_i - \max_J(A_J) \quad (2)$$

517 The model's gaze bias mechanism is implemented in the absolute evidence signal A_i :
518 Similar to the aDDM, the absolute evidence signals are assumed to be proportional to the
519 value ratings r_i , and crucially, switch between two different states during the trial: an
520 unbiased state, when an item is currently looked at, and a biased state, when gaze is directed

521 towards a different item. Therefore, on average, A_i is a linear combination of two terms that
522 are weighted by the fraction g_i of the total fixation time that item i was fixated in the trial:

$$523 \quad A_i = g_i \times r_i + (1 - g_i) \times \gamma r_i \quad (3)$$

524 Here, γ ($-1 \leq \gamma \leq 1$) is the model's gaze bias parameter that determines the strength of
525 the downweighting during the biased state. If $\gamma = 1$, there is no difference between the biased
526 and unbiased state, producing no gaze bias. If $\gamma < 1$, the absolute evidence signal is discounted
527 by the γ parameter, resulting in a gaze bias. If $-1 \leq \gamma < 0$, the sign of the evidence signal
528 changes, thereby leaking evidence, when the item is not fixated. This leakage mechanism is
529 supported by a recent empirical study (Ashby et al., 2016). The maximum amount of evidence
530 that can be accumulated or leaked at each time point is symmetric in magnitude, as the γ
531 parameter is bounded between -1 and 1.

532 Note that the range of possible R_i^* (equation (2)) depends on the participants' use of
533 the item rating scale: if the ratings only cover a narrow range of possible values on the scale,
534 the relative evidence values R_i^* will likewise be small, whereas they will be large if the
535 participant utilizes the entire range of the rating scale. GLAM assumes an adaptive
536 representation of the relative evidence signals that is compensating for the participants' use of
537 the rating scale and thereby sensitive to marginal differences in the relative evidences,
538 particularly to values close to 0 (where the absolute evidence signal for one item is only
539 marginally different to the maximum of all others). To this end, a logistic transform $s(x)$,
540 with scaling parameter τ is applied:

$$541 \quad s(x) = \frac{1}{1 + \exp(-\tau x)} \quad (4)$$

$$542 \quad R_i = s(R_i^*) \quad (5)$$

543 The first passage time density $f_i(t)$ of a single linear stochastic accumulator E_i , with
544 decision boundary b , is given by the Inverse Gaussian Distribution (Wald, 1973):

$$545 \quad f_i(t) = \left[\frac{\lambda}{2\pi t^3} \right]^{1/2} \exp \left\{ \frac{-\lambda(t-\mu)^2}{2\mu^2 t} \right\} \text{ with } \mu = \frac{b}{vR_i} \text{ and } \lambda = \frac{b^2}{\sigma^2} \quad (6)$$

546 However, this density does not take into account that there are multiple accumulators
547 in each trial racing towards the same boundary. As soon as any of these accumulators crosses
548 the boundary a choice is made and the trial ends. For this reason, $f_i(t)$ must be corrected for
549 the probability that any other accumulator crosses the boundary first. The probability that a
550 single accumulator crosses the boundary prior to t , is given by its cumulative distribution
551 function $F_i(t)$:

$$552 \quad F_i(t) = \Phi\left(\sqrt{\frac{\lambda}{t}}\left(\frac{t}{\mu} - 1\right)\right) + \exp\left(\frac{2\lambda}{\mu}\right) \Phi\left(-\sqrt{\frac{\lambda}{t}}\left(\frac{t}{\mu} + 1\right)\right), \quad (7)$$

553 where $\Phi(x)$ is the standard normal cumulative distribution function. Hence, the joint
554 probability $p_i(t)$ that accumulator E_i crosses b at time t , and that no other accumulator j has
555 reached b first, is given by:

$$556 \quad p_i(t) = f_i(t) \prod_j (1 - F_j(t)). \quad (8)$$

557 We performed a parameter recovery study to rule out misspecifications of the model
558 and assert the validity of the parameters estimated from empirical data. All of the parameters
559 could be recovered to a satisfying degree (see [Figure S1](#) for detailed results).

560 Although the race framework deviates from the classical Drift-Diffusion Model
561 (DDM; Ratcliff, 1978; Ratcliff et al., 2016), which is known to implement an optimal
562 decision procedure in the sense of the sequential probability ratio test (Bogacz, Brown,
563 Moehlis, Holmes, & Cohen, 2006), it has reasonable benefits in the context of this paper: first,
564 the model naturally generalizes to choices between three alternatives, which is not trivial for
565 the classical DDM. Second, it generalizes to settings with even larger choice sets. Third, an
566 analytical solution for the first-passage time density of the linear stochastic race exists. This
567 solution enables a very fast and efficient parameter estimation, without the need to
568 numerically estimate densities from a large number of model simulations.

569

570

571 **GLAM parameter estimation**

572 **Individual.** For the individual model comparison, we first estimated the model
573 parameters at the individual level. The full GLAM has four parameters (ν , γ , σ , τ). The
574 individual models were implemented in the Python library PyMC3 (Salvatier, Wiecki, &
575 Fonnesbeck, 2016) and fitted using the default Markov Chain Monte Carlo No-U-Turn-
576 Sampler (NUTS; Hoffman & Gelman, 2014). We parameterized the model so that the noise
577 parameter σ was sampled proportionally to the velocity parameter ν using a signal-to-noise
578 variable SNR (note that this does not add a free parameter to the model, as σ is now fully
579 determined by ν and SNR). We placed uninformative, uniform priors between sensible limits
580 on all model parameters:

581 $\nu \sim \text{Uniform}(1e-10, 0.01)$

582 $\gamma \sim \text{Uniform}(-1, 1)$

583 $SNR \sim \text{Uniform}(1, 500)$

584 $\sigma = \nu \times SNR$

585 $\tau \sim \text{Uniform}(0, 5)$

586 Further, we assumed a fixed 5% rate of error trials, which we model as a participant-
587 specific uniform likelihood distribution $u_s(t)$. This error likelihood describes the probability
588 of a random choice for any of the N available choice items at a random time point in the
589 interval of empirically observed response times (cf. Ratcliff & Tuerlinckx, 2002; Wiecki et
590 al., 2013):

591
$$u_s(t) = \frac{1}{N(\max(rt_s) - \min(rt_s))} \quad (9)$$

592 The resulting choice likelihood is then given by:

593
$$l_i(t) = 0.95 \times p_i(t) + 0.05 \times u_s(t) \quad (10)$$

594 For each individual model, the NUTS sampler was initialized using the default
595 behavior in PyMC 3.2, followed by 500 tuning samples that were discarded. Finally, we drew
596 2000 posterior samples that we used to estimate the model parameters.

597 In addition, a restricted no-gaze-bias GLAM variant was also fit to the individual data.
598 It was specified and fitted identically to the full model, but had the gaze-bias parameter γ fixed
599 at 1.0. The reported parameter estimates are maximum a posteriori (MAP) estimates.

600 **Hierarchical.** We also estimated the GLAM parameters in a hierarchical Bayesian
601 framework (Kruschke, 2014; Vandekerckhove, Tuerlinckx, & Lee, 2008; Wiecki et al., 2013).
602 Here, the fit of participant level parameters is informed by the group distribution of
603 parameters. Each parameter on the participant level is modeled as coming from a population
604 distribution whose shape and location are also estimated from the data. We assumed that all
605 participant level parameters are drawn from normal population distributions, which we
606 bounded to sensible ranges:

607
$$v \in (1e-10, 0.01), SNR \in (1, 500), \gamma \in (-1, 1), \tau \in (0, 5).$$

608 We used ADVI (Kucukelbir, Ranganath, Gelman, & Blei, 2015) from the PyMC3
609 python library (Salvatier et al., 2016) to approximate the posterior distribution of the model
610 parameters. In analogy to the individual models, we assumed a fixed 5% rate of participant-
611 specific uniformly distributed error responses (see above). The reported parameter estimates
612 are maximum a posteriori (MAP) estimates.

613

614 **Model simulations**

615 Choice and response time data was simulated from the GLAM according to the
616 following procedures: each trial in the left-out data set, containing all the odd-numbered trials,
617 was repeated 50 times. For every trial the model used the empirically observed item ratings
618 and gaze distributions. With a fixed rate of 5% the simulation produced a random choice and
619 a random response time between the participant's minimum and maximum observed response

620 times (cf. equations (9) & (10)). With a rate of 95% the choice and response time were
621 simulated from the actual GLAM: for each item in the trial, a first passage time (FPT) was
622 drawn according to the single-item first passage densities (equation (8)). The response time
623 and choice were then determined by the item with the shortest FPT.

624

625 **Availability of data, model and analysis code**

626 All analyses and figures can be reproduced using the data set, scripts and GLAM
627 resources that are available at <http://www.github.com/glamlab/glam>.

628

629 **Software**

630 All analyses were performed in Python, using the NumPy and SciPy (Van der Walt,
631 Colbert & Varoquaux, 2011), Pandas (McKinney, 2010), Statsmodels (Skipper & Perktold,
632 2010), PyMC3 (Salvatier et al., 2016) and Theano (Theano Development Team, 2016)
633 libraries. We used Matplotlib (Hunter, 2007) for visualization.

634

635 **References**

- 636 Armel, K. C., Beaumel, A., & Rangel, A. (2008). Biasing simple choices by manipulating
637 relative visual attention. *Judgment and Decision Making*, 3(5), 396-403.
- 638 Ashby, N. J. S., Jekel, M., Dickert, S., & Glöckner, A. (2016). Finding the right fit: A
639 comparison of process assumptions underlying popular drift-diffusion models. *Journal*
640 *of Experimental Psychology: Learning, Memory, and Cognition*, 42(12), 1982-1993.
641 <http://doi.org/10.1037/xlm0000279>
- 642 Basten, U., Biele, G., Heekeren, H. R., & Fiebach, C. J. (2010). How the brain integrates costs
643 and benefits during decision making. *Proceedings of the National Academy of*
644 *Sciences*, 107(50), 21767-21772. <http://doi.org/10.1073/pnas.0908104107>
- 645 Bogacz, R., Brown, E., Moehlis, J., Holmes, P., & Cohen, J. D. (2006). The physics of
646 optimal decision making: A formal analysis of models of performance in two-
647 alternative forced-choice tasks. *Psychological Review*, 113(4), 700-765.
648 <http://doi.org/10.1037/0033-295X.113.4.700>
- 649 Cavanagh, J. F., Wiecki, T. V., Kochar, A., & Frank, M. J. (2014). Eye tracking and
650 pupillometry are indicators of dissociable latent decision processes. *Journal of*
651 *Experimental Psychology: General*, 143(4), 1476-1488.
652 <http://doi.org/10.1037/a0035813>
- 653 Chandon, P., Hutchinson, J. W., Bradlow, E. T., & Young, S. H. (2009). Does in-store
654 marketing work? Effects of the number and position of shelf facings on brand
655 attention and evaluation at the point of purchase. *Journal of Marketing*, 73(6), 1-17.
656 <http://doi.org/10.1509/jmkg.73.6.1>
- 657 Churchland, A. K., Kiani, R., & Shadlen, M. N. (2008). Decision-making with multiple
658 alternatives. *Nature Neuroscience*, 11(6), 693-702. <http://doi.org/10.1038/nn.2123>
- 659 Fiedler, S., & Glöckner, A. (2012). The dynamics of decision making in risky choice: An eye-
660 tracking analysis. *Frontiers in Psychology*, 3. <http://doi.org/10.3389/fpsyg.2012.00335>

- 661 Fisher, G. (2017). An attentional drift diffusion model over binary-attribute choice. *Cognition*,
662 168, 34–45. <http://doi.org/10.1016/j.cognition.2017.06.007>
- 663 Folke, T., Jacobsen, C., Fleming, S. M., & De Martino, B. (2016). Explicit representation of
664 confidence informs future value-based decisions. *Nature Human Behaviour*, 1.
665 <http://doi.org/10.1038/s41562-016-0002>
- 666 Glöckner, A., & Herbold, A.-K. (2011). An eye-tracking study on information processing in
667 risky decisions: Evidence for compensatory strategies based on automatic processes.
668 *Journal of Behavioral Decision Making*, 24(1), 71–98. <http://doi.org/10.1002/bdm.684>
- 669 Gluth, S., & Rieskamp, J. (2017). Variability in behavior that cognitive models do not explain
670 can be linked to neuroimaging data. *Journal of Mathematical Psychology*, 76, 104–
671 116. <https://doi.org/10.1016/j.jmp.2016.04.012>
- 672 Gold, J. I., & Shadlen, M. N. (2001). Neural computations that underlie decisions about
673 sensory stimuli. *Trends in Cognitive Sciences*, 5(1), 10–16.
674 [https://doi.org/10.1016/S1364-6613\(00\)01567-9](https://doi.org/10.1016/S1364-6613(00)01567-9)
- 675 Grandy, T., Lindenberger, U., & Werkle-Bergner, M. (2017, April 11). When group means
676 fail: Can one size fit all? *bioRxiv*. <https://doi.org/10.1101/126490>
- 677 Hayes, K. J. (1953). The backward curve: A method for the study of learning. *Psychological*
678 *Review*, 60(4), 269-275. <http://doi.org/10.1037/h0056308>
- 679 Heekeren, H. R., Marrett, S., & Ungerleider, L. G. (2008). The neural systems that mediate
680 human perceptual decision making. *Nature Reviews Neuroscience*, 9(6), 467–479.
681 <http://doi.org/10.1038/nrn2374>
- 682 Hoffman, M. D., & Gelman, A. (2014). The No-U-turn sampler: Adaptively setting path
683 lengths in Hamiltonian Monte Carlo. *Journal of Machine Learning Research*, 15(1),
684 1593–1623.

- 685 Hunt, L. T., Malalasekera, W. M. N., Berker, A. O. de, Miranda, B., Farmer, S. F., Behrens,
686 T. E. J., & Kennerley, S. W. (2017, August 1). Triple dissociation of attention and
687 decision computations across prefrontal cortex. *bioRxiv*. <http://doi.org/10.1101/171173>
- 688 Hunter, J. D. (2007). Matplotlib: a 2D graphics environment. *Computing in Science &*
689 *Engineering*, 9, 90-95. <https://doi.org/10.1109/MCSE.2007.55>
- 690 Itti, L., & Koch, C. (2000). A saliency-based search mechanism for overt and covert shifts of
691 visual attention. *Vision Research*, 40(10), 1489–1506. [https://doi.org/10.1016/S0042-](https://doi.org/10.1016/S0042-6989(99)00163-7)
692 [6989\(99\)00163-7](https://doi.org/10.1016/S0042-6989(99)00163-7)
- 693 Konovalov, A., & Krajbich, I. (2016). Gaze data reveal distinct choice processes underlying
694 model-based and model-free reinforcement learning. *Nature Communications*, 7.
695 <http://doi.org/10.1038/ncomms12438>
- 696 Krajbich, I., & Rangel, A. (2011). Multialternative drift-diffusion model predicts the
697 relationship between visual fixations and choice in value-based decisions. *Proceedings*
698 *of the National Academy of Sciences*, 108(33), 13852–13857.
699 <http://doi.org/10.1073/pnas.1101328108>
- 700 Krajbich, I., Armel, C., & Rangel, A. (2010). Visual fixations and the computation and
701 comparison of value in simple choice. *Nature Neuroscience*, 13(10), 1292–1298.
702 <http://doi.org/10.1038/nn.2635>
- 703 Krajbich, I., Lu, D., Camerer, C., & Rangel, A. (2012). The attentional drift-diffusion model
704 extends to simple purchasing decisions. *Frontiers in Psychology*, 3.
705 <http://doi.org/10.3389/fpsyg.2012.00193>
- 706 Kruschke, J. (2014). *Doing Bayesian data analysis: A tutorial with R, JAGS, and Stan*.
707 Academic Press.
- 708 Kucukelbir, A., Ranganath, R., Gelman, A., & Blei, D. (2015). Automatic variational
709 inference in Stan. In *Advances in Neural Information Processing Systems* (pp. 568-
710 576).

- 711 de Lafuente, V., Jazayeri, M., & Shadlen, M. N. (2015). Representation of accumulating
712 evidence for a decision in two parietal areas. *Journal of Neuroscience*, 35(10), 4306-
713 4318. <https://doi.org/10.1523/JNEUROSCI.2451-14.2015>
- 714 Lewandowsky, S., & Farrell, S. (2010). *Computational modeling in cognition: Principles and*
715 *practice*. Sage Publications.
- 716 Liu, T., & Pleskac, T. J. (2011). Neural correlates of evidence accumulation in a perceptual
717 decision task. *Journal of Neurophysiology*, 106(5), 2383-2398.
718 <http://doi.org/10.1152/jn.00413.2011>
- 719 Lohse, G. L. (1997). Consumer eye movement patterns on yellow pages advertising. *Journal*
720 *of Advertising*, 26(1), 61–73. <https://doi.org/10.1080/00913367.1997.10673518>
- 721 De Martino, B., Bobadilla-Suarez, S., Nouguchi, T., Sharot, T., & Love, B. C. (2017). Social
722 information is integrated into value and confidence judgments according to its
723 reliability. *Journal of Neuroscience*, 37(25), 6066-6074.
724 <https://doi.org/10.1523/JNEUROSCI.3880-16.2017>
- 725 McGinty, V. B., Rangel, A., & Newsome, W. T. (2016). Orbitofrontal Cortex Value Signals
726 Depend on Fixation Location during Free Viewing. *Neuron*, 90(6), 1299-1311.
727 <https://doi.org/10.1016/j.neuron.2016.04.045>
- 728 McKinney, W. (2010, June). Data structures for statistical computing in Python. In
729 *Proceedings of the 9th Python in Science Conference* (Vol. 445, pp. 51-56). Austin,
730 TX.
- 731 Mohr, P. N. C., Heekeren, H. R., & Rieskamp, J. (2017). Attraction Effect in Risky Choice
732 Can Be Explained by Subjective Distance Between Choice Alternatives. *Scientific*
733 *Reports*, 7(1), 8942. <http://doi.org/10.1038/s41598-017-06968-5>
- 734 Noguchi, T., & Stewart, N. (2014). In the attraction, compromise, and similarity effects,
735 alternatives are repeatedly compared in pairs on single dimensions. *Cognition*, 132(1),
736 44-56. <https://doi.org/10.1016/j.cognition.2014.03.006>

- 737 Nunez, M. D., Srinivasan, R., & Vandekerckhove, J. (2015). Individual differences in
738 attention influence perceptual decision making. *Frontiers in Psychology*, 8.
739 <http://doi.org/10.3389/fpsyg.2015.00018>
- 740 Nunez, M. D., Vandekerckhove, J., & Srinivasan, R. (2017). How attention influences
741 perceptual decision making: Single-trial EEG correlates of drift-diffusion model
742 parameters. *Journal of Mathematical Psychology*, 76, 117-130.
743 <https://doi.org/10.1016/j.jmp.2016.03.003>
- 744 O'Connell, R. G., Dockree, P. M., & Kelly, S. P. (2012). A supramodal accumulation-to-
745 bound signal that determines perceptual decisions in humans. *Nature*
746 *Neuroscience*, 15(12), 1729-1735. <http://doi.org/10.1038/nn.3248>
- 747 Pärnamets, P., Johansson, P., Hall, L., Balkenius, C., Spivey, M. J., & Richardson, D. C.
748 (2015). Biasing moral decisions by exploiting the dynamics of eye gaze. *Proceedings*
749 *of the National Academy of Sciences*, 112(13), 4170-4175.
750 <http://doi.org/10.1073/pnas.1415250112>
- 751 Peters, J., & Büchel, C. (2011). The neural mechanisms of inter-temporal decision-making:
752 understanding variability. *Trends in Cognitive Sciences*, 15(5), 227-23.
753 <https://doi.org/10.1016/j.tics.2011.03.002>
- 754 Philiastides, M. G., & Sajda, P. (2007). EEG-informed fMRI reveals spatiotemporal
755 characteristics of perceptual decision making. *Journal of Neuroscience*, 27(48),
756 13082-13091. <https://doi.org/10.1523/JNEUROSCI.3540-07.2007>
- 757 Polanía, R., Krajbich, I., Grueschow, M., & Ruff, C. C. (2014). Neural oscillations and
758 synchronization differentially support evidence accumulation in perceptual and value-
759 based decision making. *Neuron*, 82(3), 709-720.
760 <https://doi.org/10.1016/j.neuron.2014.03.014>
- 761 Ratcliff, R. (1978). A theory of memory retrieval. *Psychological Review*, 85(2), 59.
762 <http://doi.org/10.1037/0033-295X.85.2.59>

- 763 Ratcliff, R., Smith, P. L., Brown, S. D., & McKoon, G. (2016). Diffusion decision model:
764 current issues and history. *Trends in Cognitive Sciences*, 20(4), 260-281.
765 <https://doi.org/10.1016/j.tics.2016.01.007>
- 766 Ratcliff, R., & Tuerlinckx, F. (2002). Estimating parameters of the diffusion model:
767 Approaches to dealing with contaminant reaction times and parameter
768 variability. *Psychonomic Bulletin & Review*, 9(3), 438-481.
769 <https://doi.org/10.3758/BF03196302>
- 770 Reutskaja, E., Nagel, R., Camerer, C. F., & Rangel, A. (2011). Search dynamics in consumer
771 choice under time pressure: An eye-tracking study. *American Economic Review*, 101,
772 900-926. <http://doi.org/10.1257/aer.101.2.900>
- 773 Rieskamp, J. (2008). The probabilistic nature of preferential choice. *Journal of Experimental*
774 *Psychology: Learning, Memory, and Cognition*, 34(6), 1446.
775 <http://doi.org/10.1037/a0013646>
- 776 Roe, R. M., Busemeyer, J. R., & Townsend, J. T. (2001). Multialternative decision field
777 theory: A dynamic connectionist model of decision making. *Psychological*
778 *Review*, 108(2), 370. <http://doi.org/10.1037/0033-295X.108.2.370>
- 779 Salvatier, J., Wiecki, T. V., & Fonnesbeck, C. (2016). Probabilistic programming in Python
780 using PyMC3. *PeerJ Computer Science*, 2, e55. <http://doi.org/10.7717/peerj-cs.55>
- 781 Seabold, S., & Perktold, J. (2010, June). Statsmodels: Econometric and statistical modelling
782 with Python. In *Proceedings of the 9th Python in Science Conference* (Vol. 57, p. 61)
- 783 Shimojo, S., Simion, C., Shimojo, E., & Scheier, C. (2003). Gaze bias both reflects and
784 influences preference. *Nature Neuroscience*, 6(12), 1317-1322.
785 <http://doi.org/10.1038/nn1150>
- 786 Soltani, A., De Martino, B., & Camerer, C. (2012). A range-normalization model of context-
787 dependent choice: a new model and evidence. *PLoS Computational Biology*, 8(7),
788 e1002607. <https://doi.org/10.1371/journal.pcbi.1002607>

- 789 Spiegelhalter, D. J., Best, N. G., Carlin, B. P., & van der Linde, A. (2014). The deviance
790 information criterion: 12 years on. *Journal of the Royal Statistical Society: Series B*
791 (*Statistical Methodology*), 76(3), 485-493. <https://doi.org/10.1111/rssb.12062>
- 792 Spiegelhalter, D. J., Best, N. G., Carlin, B. P., & van der Linde, A. (2002). Bayesian measures
793 of model complexity and fit. *Journal of the Royal Statistical Society: Series B*
794 (*Statistical Methodology*), 64(4), 583-639. <https://doi.org/10.1111/1467-9868.00353>
- 795 Stewart, N., Gächter, S., Noguchi, T., & Mullett, T. L. (2016). Eye movements in strategic
796 choice. *Journal of Behavioral Decision Making*, 29(2-3), 137-156.
797 <https://doi.org/10.1002/bdm.1901>
- 798 Stewart, N., Hermens, F., & Matthews, W. J. (2016). Eye movements in risky choice. *Journal*
799 *of Behavioral Decision Making*, 29(2-3), 116-136. <https://doi.org/10.1002/bdm.1854>
- 800 Tavares, G., Perona, P., & Rangel, A. (2017). The Attentional Drift Diffusion Model of
801 Simple Perceptual Decision-Making. *Frontiers in Neuroscience*, 11, 468.
802 <https://doi.org/10.3389/fnins.2017.00468>
- 803 Theano Development Team (2016). Theano: a Python framework for fast computation of
804 mathematical expressions. *arXiv*.
- 805 Tillman, G. (2017, September 18). The Racing Diffusion Model of Speeded Decision
806 Making. <http://doi.org/10.17605/OSF.IO/XUWBK>
- 807 Towal, R. B., Mormann, M., & Koch, C. (2013). Simultaneous modeling of visual saliency
808 and value computation improves predictions of economic choice. *Proceedings of the*
809 *National Academy of Sciences*, 110(40), E3858-E3867.
810 <http://doi.org/10.1073/pnas.1304429110>
- 811 Trueblood, J. S., Brown, S. D., Heathcote, A., & Busemeyer, J. R. (2013). Not just for
812 consumers: Context effects are fundamental to decision making. *Psychological*
813 *Science*, 24(6), 901-908. <https://doi.org/10.1177/0956797612464241>

- 814 Usher, M., & McClelland, J. L. (2001). The time course of perceptual choice: The leaky,
815 competing accumulator model. *Psychological Review*, 108(3), 550.
816 <http://doi.org/10.1037/0033-295X.108.3.550>
- 817 Usher, M., Olami, Z., & McClelland, J. L. (2002). Hick's law in a stochastic race model with
818 speed-accuracy tradeoff. *Journal of Mathematical Psychology*, 46(6), 704-715.
819 <https://doi.org/10.1006/jmps.2002.1420>
- 820 Vaidya, A. R., & Fellows, L. K. (2015). Testing necessary regional frontal contributions to
821 value assessment and fixation-based updating. *Nature Communications*, 6, 10120.
822 <https://doi.org/10.1038/ncomms10120>
- 823 Vandekerckhove, J., Tuerlinckx, F., & Lee, M. (2008, July). A Bayesian approach to
824 diffusion process models of decision-making. In *Proceedings of the 30th Annual*
825 *Conference of the Cognitive Science Society* (pp. 1429-1434). Cognitive Science
826 Society.
- 827 Von Neumann, J., & Morgenstern, O. (1945). *Theory of games and economic behavior*.
828 Princeton, NJ: Princeton University Press.
- 829 Wald, A. (1973). *Sequential analysis*. Courier Corporation.
- 830 van der Walt, S., Colbert, S., C., & Varoquaux, G (2011). The NumPy Array: A Structure for
831 Efficient Numerical Computation. *Computing in Science & Engineering*, 13, 22-30.
832 <http://doi.org/10.1109/MCSE.2011.37>
- 833 Wedel, M., & Pieters, R. (2008). A review of eye-tracking research in marketing. In *Review of*
834 *marketing research* (pp. 123-147). Emerald Group Publishing Limited.
- 835 Wiecki, T. V., Sofer, I., & Frank, M. J. (2013). HDDM: Hierarchical Bayesian estimation of
836 the drift-diffusion model in Python. *Frontiers in Neuroinformatics*, 7.
837 <http://doi.org/10.3389/fninf.2013.00014>

- 838 Wyart, V., De Gardelle, V., Scholl, J., & Summerfield, C. (2012). Rhythmic fluctuations in
839 evidence accumulation during decision making in the human brain. *Neuron*, 76(4),
840 847-858. <https://doi.org/10.1016/j.neuron.2012.09.015>

841

Acknowledgements

842

Peter N. C. Mohr is funded by the Freie Universität Berlin within the Excellence

843

Initiative of the German Research Foundation (DFG). Further funding is provided by the

844

WZB Berlin Social Science Center. Armin W. Thomas is funded by the Bernstein Center for

845

Computational Neuroscience Berlin (BCCN). Felix Molter is supported by the International

846

Max Planck Research School on the Life Course (LIFE). Ian Krajbich is funded by National

847

Science Foundation Career Award 1554837.

848

849

Author contributions

850

A.W.T, F.M., H.R.H. and P.N.C.M. conceived the study. A.W.T. and F.M. designed

851

the model and carried out the data analysis. A.W.T, F.M., I.K., H.R.H. and P.N.C.M. co-

852

wrote the manuscript.

853

854

Competing interest statement

855

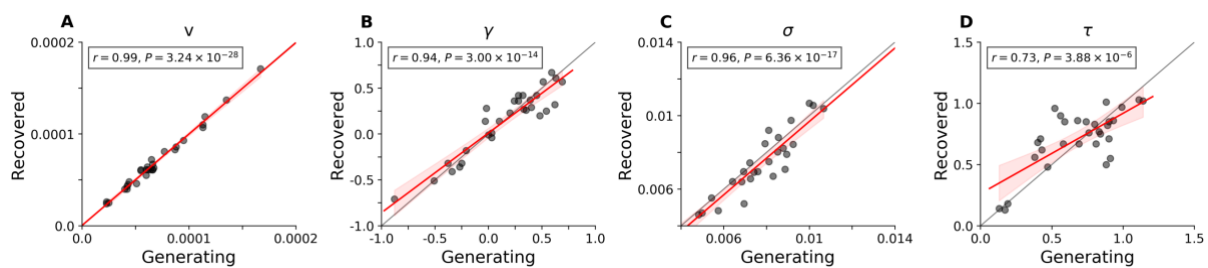
The authors declare no competing interests.

856

857

Supplementary Information

858 Parameter recovery



859

860 *Figure S1*: Results of a parameter recovery study of the GLAM. Parameter estimates

861 were estimated from model simulated data sets. Panels **A** to **D** show relationships between

862 generating and recovered parameters. All parameters could be recovered to a satisfying

863 degree.

864 We performed a parameter recovery study to validate the parameter estimates. We simulated

865 data using the GLAM and the corresponding hierarchically estimated individual parameter

866 estimates. Each empirically observed even-numbered trial (i.e., set of item value ratings and

867 relative gazes in training set trials) was simulated once, resulting in a GLAM-generated data

868 set that matches the original training data in size and structure. We then performed the exact

869 same hierarchical parameter estimation procedure as we did in the training data. Ideally, the

870 recovered parameters should match the originally estimated ones. The correlations between

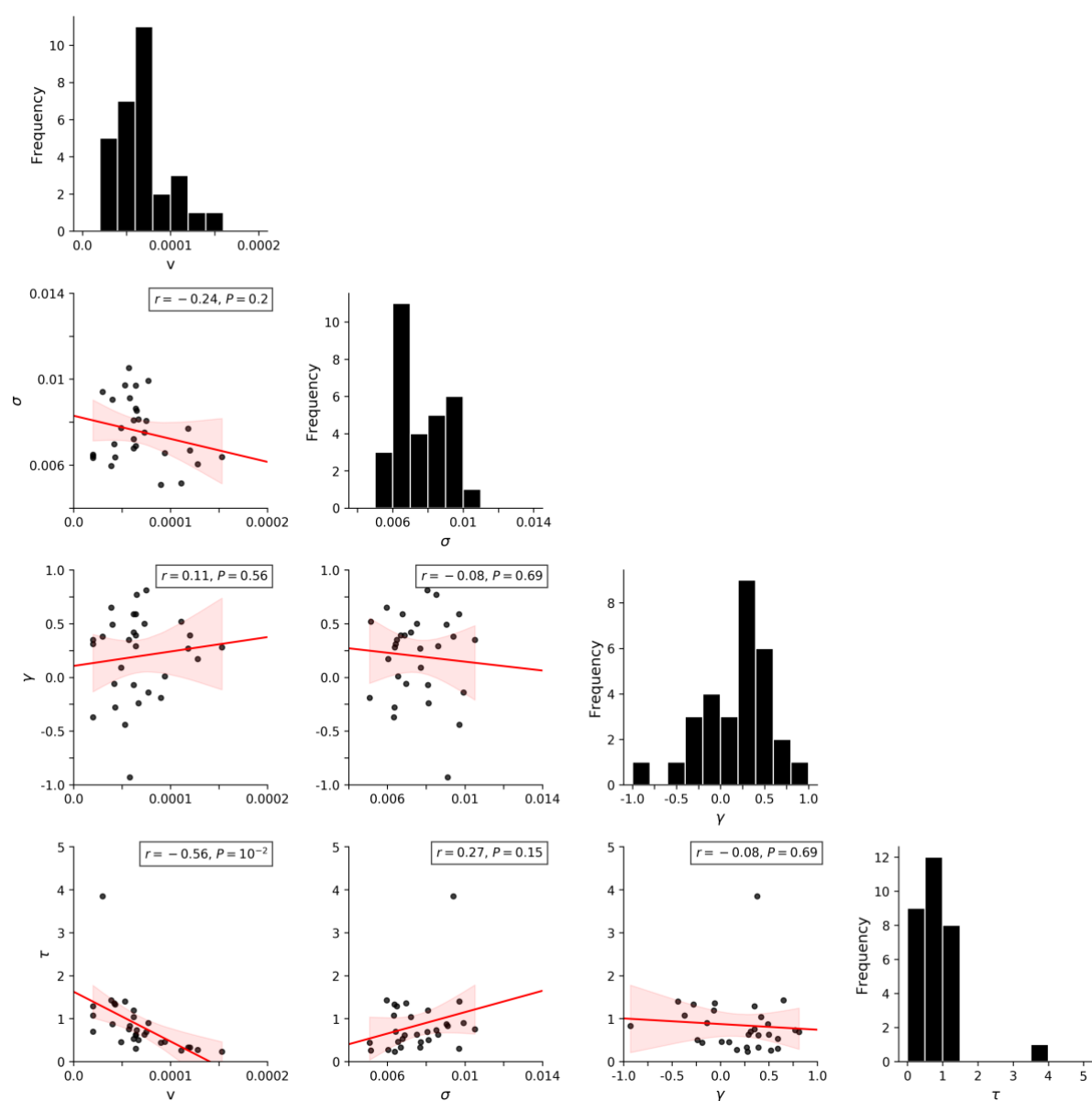
871 generating and recovered parameters are displayed in [Figure S1](#). The critical model

872 parameters v , γ and σ were recovered very well ([Figure S1 A, B, C](#), respectively). We found a

873 significant linear relationship between generating and recovered τ parameters ([Figure S1D](#)),

874 although they include some level of variance.

875 **Parameter estimates**



876

877 *Figure S2: Parameter estimates and correlations between parameters. Estimates shown*

878 *are from individual model fits.*